Journal of Dental Sciences (2015) 10, 190—200

Available online at www.sciencedirect.com

ScienceDirect

journal homepage: www.e-jds.com

ORIGINAL ARTICLE

Difference of natural teeth and implant-supported restoration: A comparison of bone remodeling simulations

Chao Wang [a,b], Gang Fu [a*], Feng Deng [a,b]

[a] College of Stomatology, Chongqing Medical University, Chongqing, China
[b] Chongqing Key Laboratory of Oral Diseases and Biomedical Sciences, Chongqing, China

Received 16 September 2014; Final revision received 13 November 2014
Available online 26 January 2015

KEYWORDS
alveolar bone;
bone density distribution;
bone remodeling simulation;
dental implant;
natural tooth

Abstract *Background/purpose:* Although there are existing numerical simulation studies on biomechanical responses induced by dental implants, particular attention has not been paid to the discrepancies of alveolar bone around natural teeth and dental implants. The purpose of this study was to compare and assess the different consequences of alveolar bone remodeling before and after dental implantation.
Materials and methods: Two three-dimensional finite element (FE) models of a maxillary bone segment were developed, comprising either implant-supported dental bridgework or natural teeth. A set of three-dimensional orthotropic bone remodeling algorithms was implemented in the FE models to analyze the stress, strain, and density distribution in the supporting bone.
Results: There were significant differences in the stress, strain, and density distribution between the intact model and implanted model. The variation of stress value was remarkably different in both models, and evident differences were found in the high stress region. Strain value was elevated in cortical bone around the implant neck, but in the intact bone strain value was distributed more evenly. In addition, bone density distribution around natural teeth was more uniform and homogeneous.
Conclusion: Simulations of adaptive bone remodeling, validated by clinical data, can be proved as a useful way to bring more insight into the mechanisms behind bone adaptation. In consideration of the crucial role of the periodontal ligament (PDL) in determining the mechanical environment in alveolar bone, it is suggested that the effect of the PDL on the bone remodeling response should be considered in future dental implant design.

* Corresponding author. Stomatological Hospital, Chongqing Medical University, 426 Songshi North Road, Chongqing, 401147, China.
E-mail address: fugang_cqdent@126.com (G. Fu).

http://dx.doi.org/10.1016/j.jds.2014.11.001

Introduction

Teeth are typically lost due to disease, accidents, the aging process, or dental decay. To replace missing teeth, a dental bridgework is usually used to restore natural function and appearance. An implant-supported restoration can provide an advanced alternative to traditional denture replacement. Benefitting from recent advances in dental implants related technology and materials, surgical placement of standard implants boasts a success rate of approximately 97% in the short term.[1,2] However, dental implant failures are generally higher in some specific groups of patients, such as patients with severe bone loss in the jawbone, periodontal disease, and bruxism problems.[3,4]

According to the classic Wolff law,[5] bone has the ability to change its internal material properties and external geometry to adapt to loads placed upon it, via a biological process called bone remodeling. During this process, bone resorption and formation are executed and regulated by bone cells (osteoclasts and osteoblasts).[6] Based on the Frost mechanostat theory,[7] bone will resorb when the mechanical loading drops below a lower threshold. When the load reaches an upper threshold values, bone apposition will occur. If the mechanical stimulus is between the upper and lower threshold values, remodeling will not take place. Moreover, where mechanical loading increases excessively, overload resorption may occur with bone loss. Changes in the mechanical loading environment due to the insertion of an implant into the jawbone have been well addressed in previous dental studies.[8–10] Therefore, in order to further improve the effectiveness of dental implants, especially over the long term, it is necessary to investigate the remodeling responses of peri-implant bone in order to obtain more detailed information about the biomechanical behavior of bone-anchored prosthetic devices.

Based on the aforementioned bone adaptation theory, some numerical studies have detailed the biomechanical responses induced by dental implants. In the field of dental biomechanics, the computational simulation of supporting bone remodeling has been carried out by previous researchers.[11,12] A bone remodeling algorithm has been developed for internal bone remodeling in the cortical and trabecular bone within jawbone. In the study by Li et al,[12] improvements in simulation methods by integrating overload bone resorption have allowed for more accurate prediction of dental implants. A study by Chou et al[13] predicted a nonhomogeneous distribution of density/elastic modulus of the mandible around various dental implant systems. Furthermore, by using a set of segmented algorithms, Lin et al[14] investigated bone remodeling around implant systems under different loading conditions, and recommended attaining proper occlusal adjustment to reduce the lateral force. Some investigators developed a series of numerical dental models correlating to clinical computed tomography (CT) data.[10,14–16] In addition, other groups focused on simulating trabecular architecture around dental implants.[17,18]

Although there are existing numerical simulation studies on biomechanical responses induced by dental implants, particular attention has not been paid to the discrepancies of alveolar bone around natural teeth and dental implants. Accordingly, more specific studies are required to qualify and quantify such differences. The objective of this work is to compare and assess the consequences of remodeling in alveolar bone before and after implantation. To achieve this, two three-dimensional (3D) finite element (FE) models of a maxillary bone segment were developed for this biomechanical analysis, comprising either the natural teeth or the three-unit implant-supported cantilever bridgework, and a set of 3D orthotropic bone remodeling algorithms were implemented herein. Furthermore, the density contours were qualitatively compared with clinical radiographic images.

Materials and methods

Finite element modeling

The 3D geometry of the maxilla was modeled from CT images of a middle-aged male patient. The CT images consisted of 312 transverse sections with a slice thickness of 0.5 mm and a pixel width of 0.398 mm. Using the software Mimics (Materialise, Leuven, Belgium) and Geomagic (Geomagic Company, NC, USA), 3D models of a segment of the maxilla (including cortical and trabecular bony structure) without teeth were built. Two FE models with natural teeth and implant-supported cantilever bridgework were constructed for evaluating the progression of bone remodeling, as shown in Fig. 1. For the intact model, two central incisors and one lateral incisor were incorporated. The periodontal ligament (PDL) was generated around the root with an average thickness of 0.2 mm. For the implanted model, a three-unit implant-supported restoration with cantilever was built. The two dental implants were 10 mm long with a diameter of 3.75 mm, based on Straumann Standard Plus Implant system (Straumann, Basel, Switzerland). The dental implants and crowns were made of titanium alloy (Ti6Al4V) and ceramics, respectively. The models were checked by a dentist to ensure the geometrical similarity, similar to previous publications.[19,20]

The models were meshed using 10-node quadratic tetrahedral elements with a global element size of 1 mm in ANSYS Workbench (Swanson Analysis System Co., Houston, TX, USA). The convergence tests for the intact and implanted models resulted in 62805 elements (nodes: 109246) and 63573 elements (nodes: 100900), respectively. Detailed elements assignments are listed in Table 1.

Occlusal mastication forces in this simulation varied for each region of the teeth. The two central incisors and lateral incisor were occlusally loaded with forces of 100 N, 100 N, and 90 N, respectively, in the buccal-lingual plane at 11° (Fig. 1). According to the actual situation, the occlusal loading forces were applied on the palatal surface about one third of crown length from incisal edge. Fully bonded interfaces were assumed between the bone and implant, simulating complete osseointegration. Moreover, the interfaces between the bones and PDL, PDL and teeth, trabecular bone and cortical bone, and abutment/implant and restoration are assumed to be perfectly bonded. As boundary conditions, the top, mesial, and distal borders of the maxilla were considered fixed to restrain all forms of movements, as shown in Fig. 1.

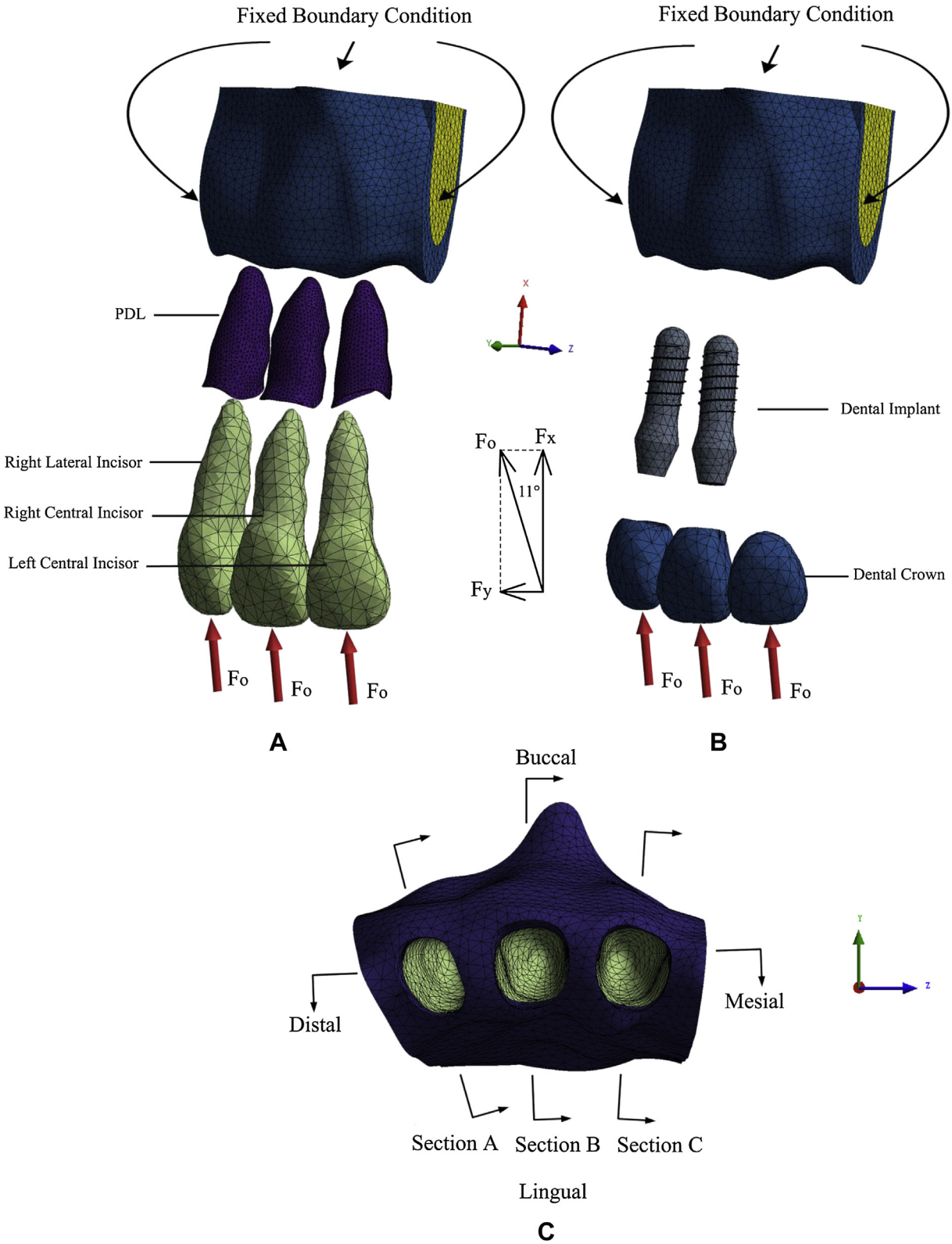

Figure 1 Finite element model of the segment of a human maxilla. (A) Intact model. (B) Implanted model. (C) Location of transverse sections used in this simulation.

The linear elastic, homogeneous, and isotropic material properties of the PDL, teeth, and implant systems are shown in Table 2. Because the mastication loading-induced strains fall in the linear elastic region of the constitutive model, the material property of the PDL was used in a linear manner. The maxillary bone was given orthotropic properties. For cortical bone,[21] the initial material properties were: $E_1 = 10.8$ GPa; $E_2 = 13.3$ GPa; $E_3 = 19.4$ GPa; $v_{12} = 0.309$ ($v_{21} = 0.381$);

Table 1 Element assignments in the finite element models.

Body name	Preoperation (intact)		Postoperation (implanted)	
	Elements	Nodes	Elements	Nodes
Cortical bone	16246	27888	15363	25751
Trabecular bone	24974	38106	37352	55769
Teeth	3290	6118	N/A	
PDL	18295	37134		
Dental implant	N/A		8131	14430
Crown	2727	4950		

$v_{23} = 0.224$ ($v_{32} = 0.328$); $v_{31} = 0.445$ ($v_{13} = 0.249$); $G_{12} = 3.81$ GPa; $G_{23} = 4.63$ GPa; $G_{31} = 4.12$ GPa. For trabecular bone,[10,22] the starting point of the algorithms is a homogeneous state of $E_1 = 3$ GPa; $E_2 = 1$ GPa; $E_3 = 0.2$ GPa, $v_{12} = v_{23} = v_{31} = 0.3$ and $G_{12} = 1.15$ GPa; $G_{23} = 0.38$ GPa; $G_{31} = 0.077$ GPa. E_1, E_2, and E_3 are elastic moduli in one, two, and three directions, G_{12}, G_{13}, G_{23} are shear moduli and v_{12}, v_{13}, v_{23} are Poisson ratios. E_1 is along the buccolingual direction; E_2 is along the inferosuperior direction; E_3 is along the mesiodistal direction. The initial density of trabecular bone and cortical bone were assumed to be 0.80 and 1.74 g/cm^3, respectively. It is noted that different bones (cortical and trabecular bone) possess different remodeling constants. In addition, the elastic moduli of both cortical and trabecular bone were updated iteratively according to the following relationship between bone density ρ (g/cm^3) and elastic moduli E_i (MPa).

For cortical bone[23]:

$$\begin{cases} E_1 = 6382 + 255(-23930 + 24000\rho) \\ E_2 = -13050 + 13000\rho \\ E_3 = -23930 + 24000\rho \end{cases} \left(1.2\ \text{g/cm}^3 \le \rho_{\text{cortical}} \le 2.0\ \text{g/cm}^3\right) \quad (1)$$

For trabecular bone:[24]

$$\begin{cases} E_1 = 2349\rho^{2.15} \\ E_2 = 1274\rho^{2.12} \\ E_3 = 194\rho \end{cases} \left(0.2\ \text{g/cm}^3 \le \rho_{\text{trabecular}} \le 1.2\ \text{g/cm}^3\right) \quad (2)$$

These concepts are outlined in Table 2.

Table 2 Material properties of the PDL, teeth and implant systems within the FE models.[14,26]

Material	Density (g/cm^3)	Elastic modulus (MPa)	Poisson ratio
Cortical bone	1.74	14700	0.30
Trabecular bone	0.80	1470	0.30
Dentine	1.20	18600	0.31
PDL	0.70	70.3	0.45
Titanium alloy implant	4.51	110000	0.35
All-ceramic FPD	5.68	140000	0.28

FPD = fixed partial denture; PDL = periodontal ligament.

Orthotropic bone remodeling calculation incorporating both underload and overload resorption

A set of orthotropic bone remodeling algorithms was employed in this study.[25,26] According to Frost's remodeling theory,[27] bone tissue can adapt its structure and properties according to different kinds of mechanical stimulus. The strain energy density (SED) was considered to be one of the most effective indicators for predicting bone remodeling.[11] The local bone density changed as a function of mechanical stimulus (SED per unit bone mass, Ψ), following the remodeling rate equations[20,28] (Equation (3a)~(3d)).

- Bone disuse resorption:

$$\frac{d\rho}{dt} = B\left(\Psi - (1-\delta)K_{ref}\right) \quad if\ \Psi < (1-\delta)K_{ref} \quad (3a)$$

- Bone equilibrium:

$$\frac{d\rho}{dt} = 0 \quad if\ (1-\delta)K_{ref} \le \Psi \le (1+\delta)K_{ref} \quad (3b)$$

- Bone formation:

$$\frac{d\rho}{dt} = B\left(\Psi - (1+\delta)K_{ref}\right) \quad if\ (1+\delta)K_{ref} < \Psi < K_{overloading} \quad (3c)$$

- Bone overload resorption:

$$\frac{d\rho}{dt} = B\left(K_{overloading} - \Psi\right) \quad if\ \Psi \ge K_{overloading} \quad (3d)$$

where Ψ denotes SED per unit bone mass (U/ρ), U is the mechanical stimulus (i.e., strain energy density herein), ρ is the bone density, B is the remodeling rate constant, K_{ref} and $K_{overloading}$ are the remodeling reference values, and δ is the bandwidth of the 'lazy zone'. As per the literature,[11,28] the input parameters can be set as B = 1.00 (g/cm^3)^2/(MPa time units), K_{ref} = 0.004 J/g, $K_{overloading}$ = 0.0358 J/g and δ = 10%. The critical overload $K_{overloading}$ is calculated from the overload threshold stress (31 MPa) and strain (4000 $\mu\varepsilon$).[28]

The ordinary differential equations (Equation (3)) were solved numerically by using the Euler method (Equation (4)), following the previous study[12]:

$$\rho^*_{n+1} = \rho_n + \Delta t f(\sigma, \rho_n) \quad (4a)$$

$$\rho_{n+1} = \rho_{n+1} + \frac{\Delta t}{2}\left[f(\sigma, \rho_n) + f\left(\sigma, \rho^*_{n+1}\right)\right] \quad (4b)$$

A small constant time step Δt (1.0e-04 $\times$ time unit) was selected to avoid large local and truncation errors.

By using Equations (3) and (4), the change in bone density with each time step was calculated. Then the corresponding elastic modulus was updated according to the relationship presented in Equations (1) and (2). The next FE analysis was then performed using the modified material properties. The iterative process was continued until the criterion for convergence was met. The bone remodeling calculation was implemented in the ANSYS and its APDL (ANSYS Parametric Design Language) programming facility, where each element was assigned an individual material property. A detailed flow chart of the remodeling procedure is provided in previous work.[20]

Results

In this simulation, equilibrium in bone density was attained after approximately 500 iterative steps. A comparison of alveolar bone response between the intact model and implanted model was performed.

Comparison of bone density contours

To represent the results of bone density distribution, different perspectives and cross-sectional views of interest were selected, as presented in Fig. 1. For the sake of clarity and readability, only the alveolar bone was shown. From the point of view outward, the bone density patterns on the cortical bone were somewhat similar. The color contours were plotted using the same scale, between 0.6 and 2.0 g/cm^3. Fig. 2 shows the contour plots for both models in the occlusal, frontal and lingual views. High-density values were noticed on the buccal and lingual side of the alveolar cortex, where density values ranged from 1.68 to 2.00 g/cm^3. Particularly, on the alveolar margin, dense bone was observed in the cervical area of both the intact bone and implanted bone, apart from a decrease in density at the rim of the cortical bone in the latter model. Overload resorption results in a slight reduction in density in this area (Fig. 2A). From the frontal view (Fig. 2B), some bone apposition (densification) was observed in the maxilla region, adjacent to the tip of the central incisor and the dental implant. A clear difference is evident where more bone densification was observed along the central dental implant as compared to the intact natural teeth model. Moreover, regarding the lingual view, different bone densification regions were noted, however, the overall density distribution was similar in both models, as shown in Fig. 2C.

From the cross-sectional views, significantly different bone density patterns can be seen between the intact and implanted alveolar bone. Subsequent to bone remodeling there was a considerable reduction in bone density in the vicinity of the dental implants. In the region of the right lateral incisor (Section A) of the alveolar bone (Fig. 3A), it can be observed that the bone density around the natural tooth was higher than that around the dental implant. In addition, around the right central incisor (Section B), bone densification occurred on both the buccal and lingual side in the intact alveolar bone, but only on the buccal side in the implanted bone (Fig. 3B). To summarize, the bone distribution around natural teeth was more uniform. Furthermore, around the left central incisor (Section C), the bone density around the natural teeth was much higher than that under the cantilever configuration (Fig. 3C).

A visual comparison between the clinical radiographs and simulated bone density distributions indicates a reasonable model validation (Fig. 4). Figs. 4A and 4B show a mesial-distal sectional view of the simulated bone distribution for both intact and implanted models. Fig. 4C shows two clinical radiographs for human natural teeth and implant-supported cantilever FPDs (Fixed Partial Dentures) embedded in the alveolar bone. From Fig. 4A (left), the high relative density can be observed between the teeth, which mirror the physiological situation, reflecting important morphological features of the alveolar bone. In contrast, low density bone between both dental implants was predicted, and higher relative density values were observed in the neighboring region of the central incisor implant, as shown in Fig. 4A (right). From the opposite direction (Fig. 4B), we can see that there was low-density bone density around implant neck in this simulation. The clinical radiographic examination indicates that there was a higher bone loss in the same region (Fig. 4C). Although bone loss varies depending on each bone type, and type of patient, it is possible to state that there is a greater possibility of bone loss. It is noted that the computational simulated results did not exhibit bone density distribution as true as in the clinical radiographs. Still, in this study, the feature differences between intact and implanted models should be our prospective goal. Hence, to a certain extent, this comparison can reflect the long term different effects of an implant-supported cantilever FPDs configuration on the bone quality, as compared with natural teeth.

Comparison of bone density values

Comparative views of the numerical results for both the intact and implanted models are presented in Figs. 5 and 6, respectively. Fig. 5 compares simulated density values in both intact and implanted alveolar bone at six sampling regions. It is worth noting that the density values in the all-root region were higher in the intact alveolar bone than in the implanted bone. In addition, it is evident that the values around the neck of natural teeth were higher in the region of both central incisors (R1 and L1) but lower in the region of the right lateral incisor (R2).Then, to compare detailed alveolar bone density distribution between the intact and implanted models, the density histology in the alveolar bone is presented in Fig. 6. Although some similarities can be observed, there was a rather different pattern of bone density histological distribution for the both models. As shown in this figure, in the range from 0.6 to 0.8 g/cm^3, density values were higher in the implanted model than in the intact model. However, in the range from 0.9 to 2.0 g/cm^3, the values were lower in the implanted model than in the intact one. Therefore, it can be concluded that retention of the natural teeth may lead to a

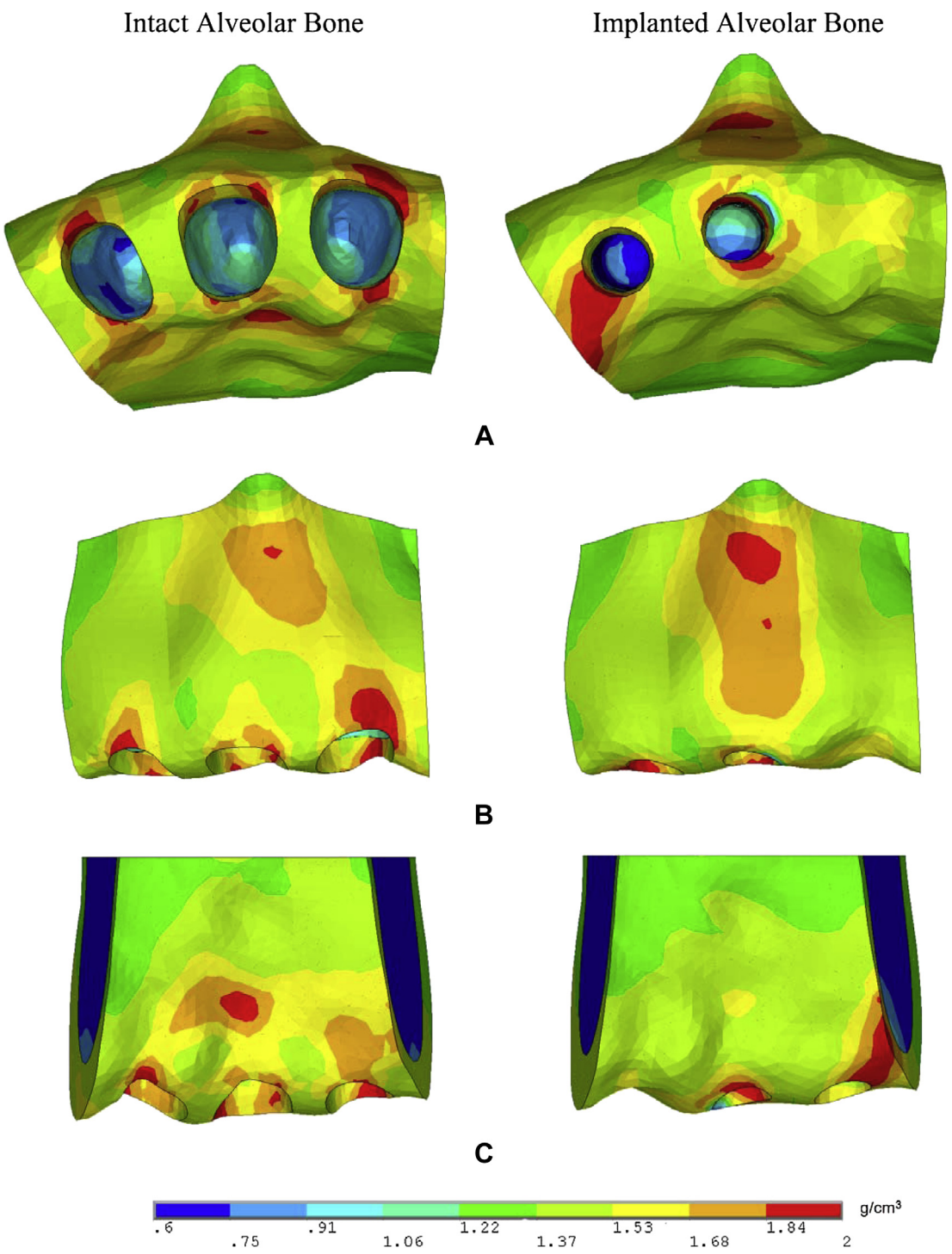

Figure 2 Comparison of simulated bone density distributions due to the bone remodeling between the intact (left) and implanted (right) model. (A) Occlusal view. (B) Frontal view. (C) Lingual view.

higher density distribution in the alveolar bone when compared with prosthetic devices.

Comparison of mechanical responses

Inserting the prosthetic component significantly altered the mechanical environment within the jaw bone. The von Mises stress value in the intact and implanted model varied from 0 to 28.25 MPa and from 0 to 30.97 MPa, respectively (Fig. 7A). The evident differences were found in the high stress region. In the intact model, high stress occurred near the cervical region of the left central incisor and in the apical region of the alveolar bone. However, for the implanted model, the stresses progressively increased from the incisory margin to the root apex along the implant longitudinal axis, and were localized circumferentially around cortical bone near to the implant neck. Concerning

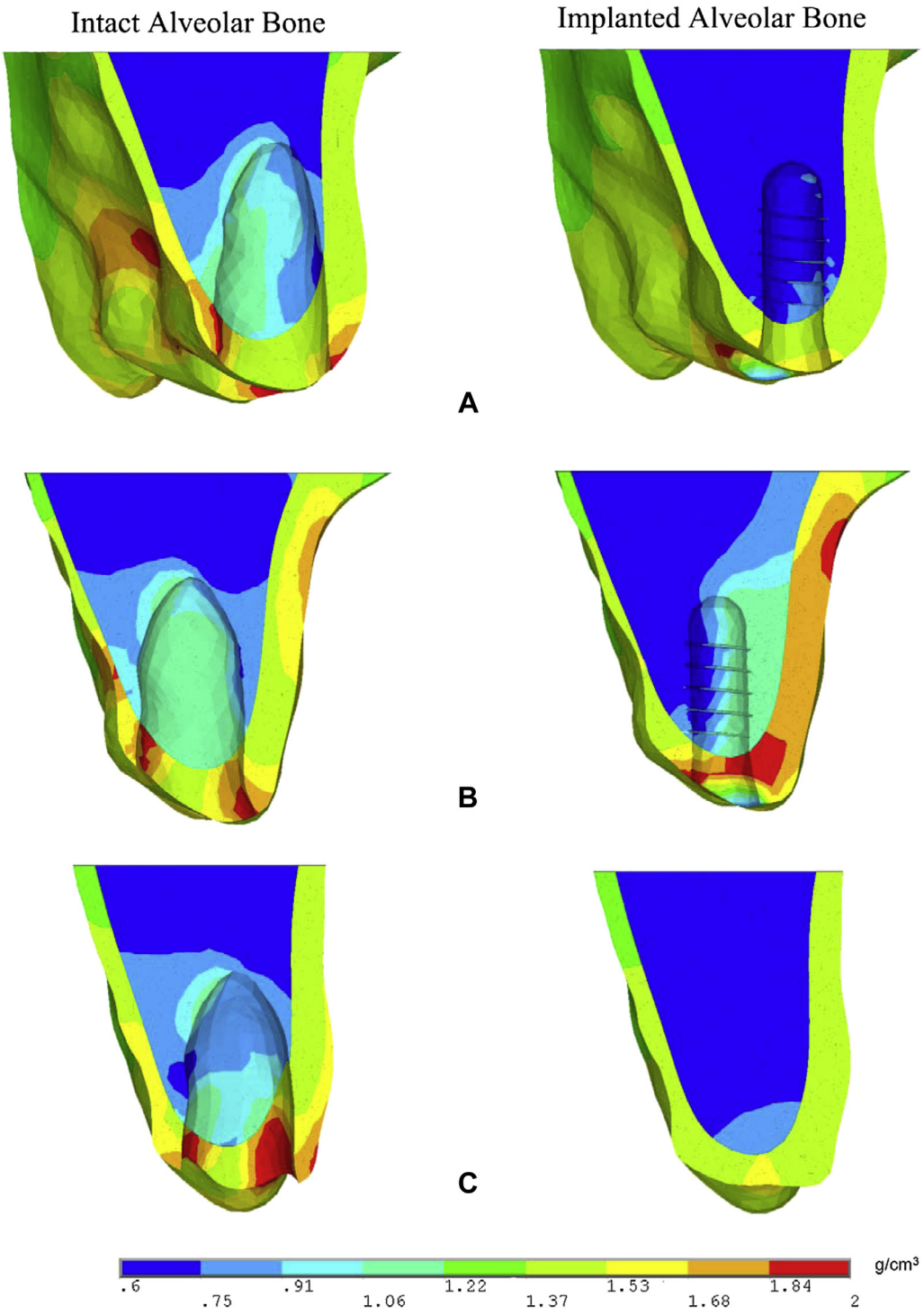

Figure 3 Different cross-sectional views of simulated bone density distribution in: intact alveolar bone (left) and implanted one (right). (A) Section A: lateral incisor region. (B) Section B: right central incisor region. (C) Section C: left central incisor region.

the von Mises strain distribution, dental implantation leaded to elevated strains around the cortical neck region. The maximal values of strain reached 0.6265%. However, these elevated strains were concentrated in a small area of bone (Fig. 7B, right). In contrast, the strain value in the intact bone was distributed more evenly than that of implanted model, as shown in Fig. 7B, left.

Discussion

In this work a computational bone remodeling model was employed to estimate the influence of the implant-supported cantilever bridgework on peri-implant bone density distribution. A set of 3D orthotropic material bone

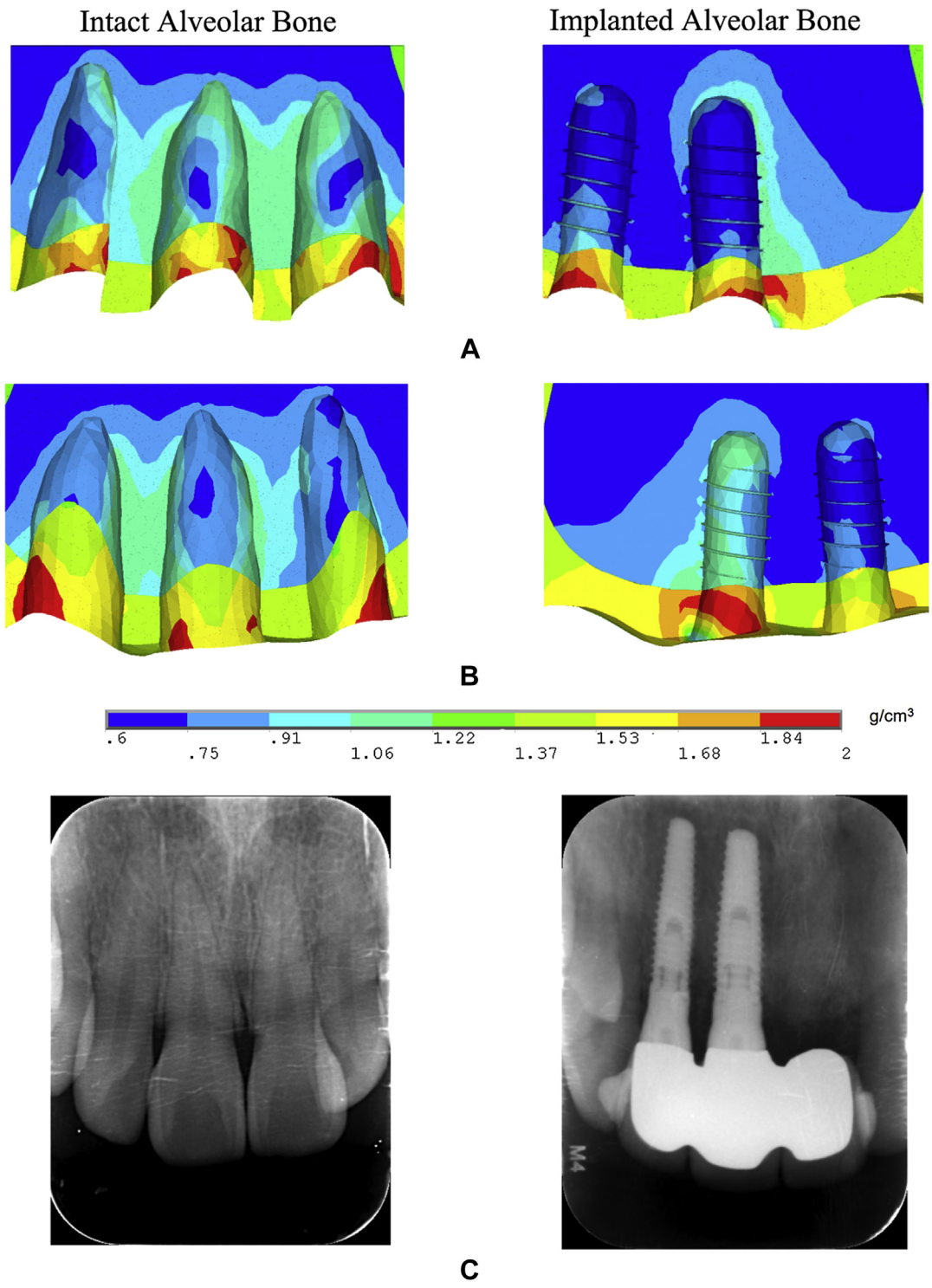

Figure 4 A mesial-distal section through the natural (left) and implanted (right) alveolar bone. Simulated bone density distribution (A) from the frontal view and (B) the lingual view. (C) Radiograph showing internal bone morphology.

remodeling algorithms was introduced. Based on the numerical results, a comparative evaluation of the bone remodeling responses can help optimize future dental implant designs and promote long-term success rate.

Among the existing mathematical models for bone remodeling around implants, almost all models assumed bone to be an isotropic material. However, real bone is anisotropic and inhomogeneous,[29] proving the isotropic assumption to be inaccurate. Available clinical and experimental evidence indicate the biomechanical behavior of maxillary bone is orthotropic. In fact, an effective orthotropic material remodeling algorithm has been developed by previous researchers,[25,26] and was implemented with the finite element method to investigate the bone remodeling

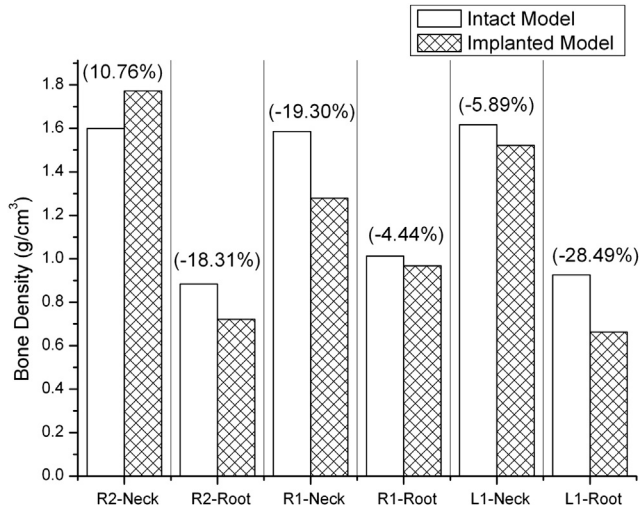

Figure 5 Comparison of simulated density values in intact and implanted maxilla at eight sampling regions. R2 = right lateral incisor region; R1 = right central incisor region; L1 = left central incisor region.

responses.[30] An orthotropic model of jawbone has been recently introduced into dental biomechanics by Aversa et al.[10] It is believed that more biofaithful results can be obtained by integrating this orthotropic assumption.

The results of this study suggested a significant difference in the bone density distribution between the intact model and implanted model. The bone density distribution around natural tooth was more uniform and homogeneous as compared to implanted alveolar bone. In our opinion, the PDL plays a very important role in the bone's responses. The PDL is a group of specialized connective tissue fibers that essentially attach a tooth to the alveolar bone.[31] From a mechanical viewpoint, the PDL functions as a shock absorber to dissipate the bite forces during mastication. These fibers can act as elastic material, allowing the tooth to homogeneously transfer load to bone during chewing.

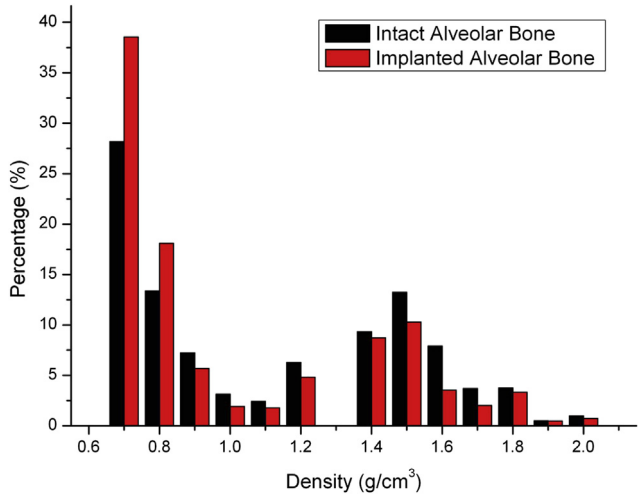

Figure 6 Histological comparison of simulated bone density in the intact and implanted alveolar bone.

That is to say, the stress/strain can be more equally distributed to alveolar bone, as shown in Fig. 7. Because the mass and strength of bone depends on its mechanical environment, the presence of a PDL improves the biomechanical performance of natural tooth in comparison with dental implant. Furthermore, due to the high elastic modulus of dental implants, a larger amount of the masticatory load was applied to the cortical neck, producing high stress/strain concentrations localized at cortical bone to implant border (Fig. 7). The bone density around dental implants is obviously lower than that around the natural tooth. According to previous clinical studies, dental implants placed in lower density bone have a higher failure rate.[1] It is thought that the altered mechanical environment from prosthetic devices could undermine (jeopardize) long-term reliability and durability.

Adding to the aforementioned discussion, an ideal load-bearing dental implant must match as close as possible the natural tooth's mechanical behavior. Although dental implants can be surgically placed in the jaw bone to replace the root of missing teeth, marginal bone loss around dental implants is inevitable, resulting in crater-like defects.[32] In the absence of the PDL, masticatory load cannot be transmitted uniformly from the tooth to the inner structure of alveolar bone. This could impair the clinical outcome of implant surgery. Furthermore, without the PDL, the periodontal mechanoreceptor feedback is absent during biting and chewing. Existing studies indicate that periodontal mechanoreceptors play a major role in the control of jaw movements and forces from food manipulation.[33] For this reason, patients with dental implants show impaired adaptation of jaw muscle activity for different food. Hence, it is necessary to take into account the effect of the PDL during implant design.

The influences of the cantilever restoration on alveolar bone remodeling consequences should be discussed. On the one hand, the incorporation of cantilever structure could aggravate the stress/strain concentrations around implant. As a result of the remodeling responses, bone density increased in the adjacent region around implant (Fig. 4). But it is noteworthy that, if biting force is more excessive (such as bruxism) than usual, marginal bone might be due to overload stress/strain which occurs clinically, increasing implant failure risk. On the other hand, it can also be observed that, for the implanted model, alveolar bone at the left central incisor region experienced a greater bone density loss, as compared with the natural teeth model. This means that bone disuse resorption occurs in this region, because most masticatory loading is borne by the cantilever extension, which can lead to a certain stress shielding within the underlying bone.

These some assumptions and limitations remain to be the biggest obstacle to accurately predict bone remodeling consequences. First, it should be pointed out that the remodeling algorithms used in this study do not take into account the individual variation of the bone density due to age, sex, and other patient-specific factors. Therefore, the effect of different patient-specific factors on the bone remodeling should be incorporated in the further work. Second, orthotropic material properties were used to take into account the bone's anisotropic nature. However, based on the bone remodeling theory, the local orientation

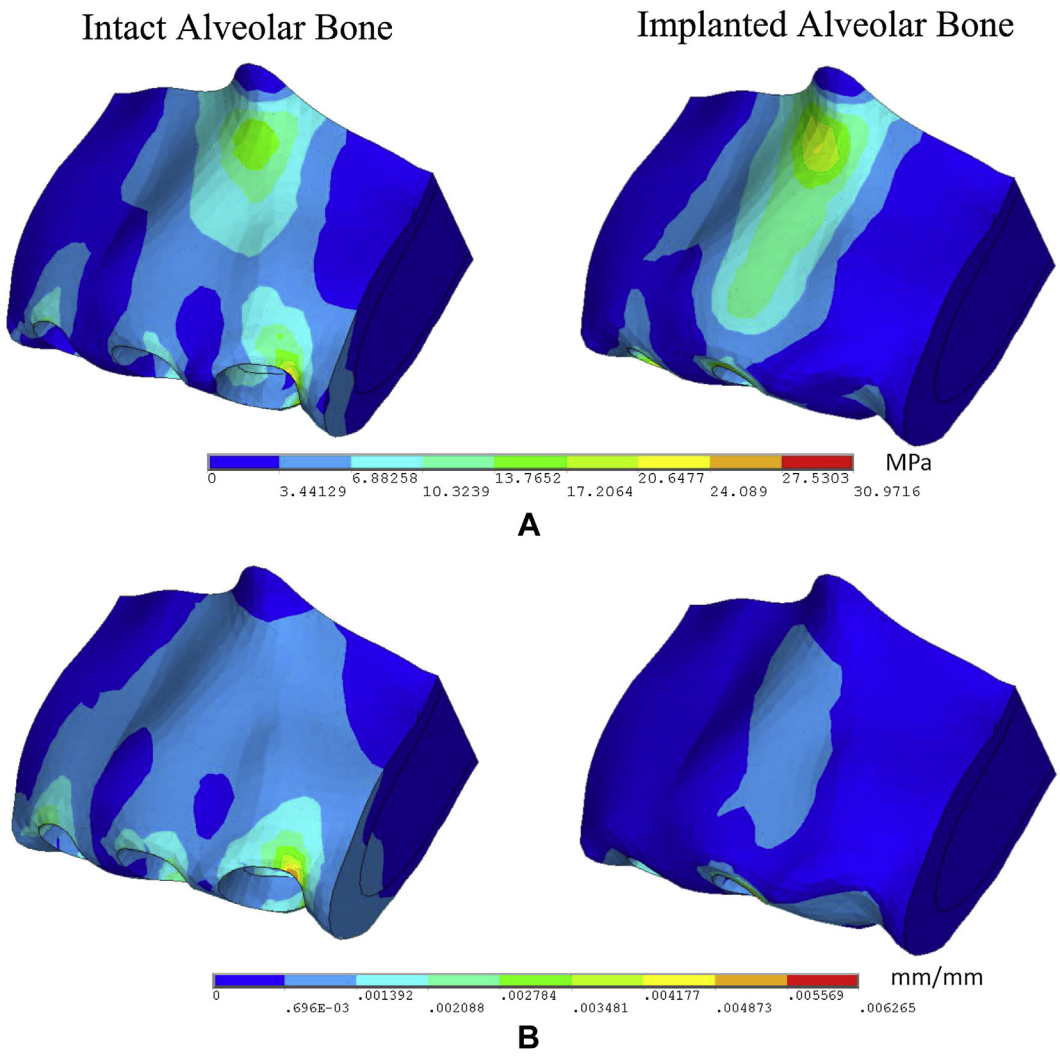

Figure 7 (A) von Mises stress and (B) von Mises strain in the intact model (left) and implanted model (right). The regional stress distribution was similar in both models, but the strain distribution was different.

and degree of anisotropy are variables that change with the external mechanical loading in trabecular bone structure.[34] Probably for this reason, the orientation of the maximum stiffness for each site should be oriented with respect to the local maximum principle stress direction. Third, the starting point of the remodeling algorithms is a homogeneous trabecular bone density distribution. In fact, trabecular bone in the maxilla is highly nonhomogeneous. Therefore, an inherent distribution of bone density in the maxilla should be initially assigned to the elements according to the grayscale of CT scanned images data. Finally, the PDL was considered as a homogeneous, isotropic, and linear elastic material. However, the PDL's naturally fibrous texture with varying principle direction around the tooth offers heterogeneous, anisotropic, and viscoelastic material properties.[31,35] Because the PDL plays a crucial role in determining the mechanical environment in alveolar bone, a more accurate computational model will be required to evaluate the alveolar bone remodeling responses.

Computer simulations of adaptive bone remodeling, validated by clinical data, are a useful way to bring more insight into the mechanisms behind bone adaptation. Accurate computational models to investigate alveolar bone remodeling before and after the placement of the three-unit implant-supported cantilever bridgework have been developed and evaluated. Different bone remodeling consequences were compared with regard to the stress, strain, and density distribution. Due to the effect of the PDL, bone density in the intact alveolar bone was more uniform and homogeneous than that of implanted model. Therefore, it is suggested that the effect of the PDL should be considered in future dental implant design. The effect of bone remodeling on the success of dental restorative surgery is critical for the development of dental implants with improved longevity. It is hoped that this comparative analysis of bone remodeling can effectively contribute to design of dental implants in the future.

Conflicts of interest

The authors have no conflicts of interest relevant to this article.

Acknowledgments

The work was supported by the National Natural Science Foundation of China (grant no. 11402042) and by the Program for Innovation Team Building at Institutions of Higher Education in Chongqing in 2013. Special thanks to Professor Yubo Fan of Beihang University at Beijing for his guidance.

References

1. Porter JA, von Fraunhofer JA. Success or failure of dental implants? A literature review with treatment considerations. *Gen Dent* 2005;53:423—32. quiz 33, 46.
2. Creugers NH, Kreulen CM, Snoek PA, de Kanter RJ. A systematic review of single-tooth restorations supported by implants. *J Dent* 2000;28:209—17.
3. Lindhe J, Karring T, Lang NP. *Clinical Periodontology and Implant Dentistry*, 4th ed. Oxford, UK: Malden, MA, Blackwell, 2003.
4. Lobbezoo F, Brouwers JE, Cune MS, Naeije M. Dental implants in patients with bruxing habits. *J Oral Rehabil* 2006;33:152—9.
5. Wolff J. *The Law of Bone Remodeling (Translation of the German 1892 Edition)*. Berlin Heidelberg New York: Springer, 1986.
6. Robling AG, Castillo AB, Turner CH. Biomechanical and molecular regulation of bone remodeling. *Annu Rev Biomed Eng* 2006;8:455—98.
7. Frost HM. Bone's mechanostat: a 2003 update. *Anat Rec A Discov Mol Cell Evol Biol* 2003;275:1081—101.
8. Rubo JH, Capello Souza EA. Finite-element analysis of stress on dental implant prosthesis. *Clin Implant Dent Relat Res* 2010;12:105—13.
9. Quaresma SE, Cury PR, Sendyk WR, Sendyk C. A finite element analysis of two different dental implants: stress distribution in the prosthesis, abutment, implant, and supporting bone. *J Oral Implant* 2008;34:1—6.
10. Aversa R, Apicella D, Perillo L, et al. Non-linear elastic three-dimensional finite element analysis on the effect of endo-crown material rigidity on alveolar bone remodeling process. *Dent Mater* 2009;25:678—90.
11. Mellal A, Wiskott HW, Botsis J, Scherrer SS, Belser UC. Stimulating effect of implant loading on surrounding bone. Comparison of three numerical models and validation by in vivo data. *Clin Oral Implants Res* 2004;15:239—48.
12. Li J, Li H, Shi L, et al. A mathematical model for simulating the bone remodeling process under mechanical stimulus. *Dent Mater* 2007;23:1073—8.
13. Chou HY, Jagodnik JJ, Muftu S. Predictions of bone remodeling around dental implant systems. *J Biomech* 2008;41:1365—73.
14. Ammar HH, Ngan P, Crout RJ, Mucino VH, Mukdadi OM. Three-dimensional modeling and finite element analysis in treatment planning for orthodontic tooth movement. *Am J Orthod Dentofacial Orthop* 2011;139:e59—71.
15. Field C, Li Q, Li W, Thompson M, Swain M. Prediction of mandibular bone remodeling induced by fixed partial dentures. *J Biomech* 2010;43:1771—9.
16. Field C, Li Q, Li W, Thompson M, Swain M. A comparative mechanical and bone remodeling study of all-ceramic posterior inlay and onlay fixed partial dentures. *J Dent* 2012;40:48—56.
17. Hasan I, Rahimi A, Keilig L, Brinkmann KT, Bourauel C. Computational simulation of internal bone remodeling around dental implants: a sensitivity analysis. *Comput Methods Biomech Biomed Engin* 2012;15:807—14.
18. Wang C, Wang L, Liu X, Fan Y. Numerical simulation of the remodeling process of trabecular architecture around dental implants. *Comput Methods Biomech Biomed Engin* 2014;17:286—95.
19. Wang C, Han J, Li Q, Wang L, Fan Y. Simulation of bone remodeling in orthodontic treatment. *Comput Methods Biomech Biomed Engin* 2014;17:1042—50.
20. Wang C, Li Q, McClean C, Fan Y. Simulated dental bone remodeling response around implant-supported fixed partial dentures with or without cantilever extension. *Int J Numer Method Biomed Eng* 2013;29:1134—47.
21. Ashman RB, Van Buskirk WC. The elastic properties of a human mandible. *Adv Dent Res* 1987;1:64—7.
22. Lowet G, Van Audekercke R, Van der Perre G, Geusens P, Dequeker J, Lammens J. The relation between resonant frequencies and torsional stiffness of long bones in vitro. Validation of a simple beam model. *J Biomech* 1993;26:689—96.
23. Rho JY, Hobatho MC, Ashman RB. Relations of mechanical properties to density and CT numbers in human bone. *Med Eng Phys* 1995;17:347—55.
24. O'Mahony AM, Williams JL, Katz JO, Spencer P. Anisotropic elastic properties of cancellous bone from a human edentulous mandible. *Clin Oral Implants Res* 2000;11:415—21.
25. Jacobs CR, Simo JC, Beaupre GS, Carter DR. Adaptive bone remodeling incorporating simultaneous density and anisotropy considerations. *J Biomech* 1997;30:603—13.
26. Miller Z, Fuchs MB, Arcan M. Trabecular bone adaptation with an orthotropic material model. *J Biomech* 2002;35:247—56.
27. Frost HM. Skeletal structural adaptations to mechanical usage (SATMU): 4. Mechanical influences on intact fibrous tissues. *Anat Rec* 1990;226:433—9.
28. Lin CL, Lin YH, Chang SH. Multi-factorial analysis of variables influencing the bone loss of an implant placed in the maxilla: prediction using FEA and SED bone remodeling algorithm. *J Biomech* 2010;43:644—51.
29. Yang G, Kabel J, van Rietbergen B, Odgaard A, Huiskes R, Cowin SC. The anisotropic Hooke's law for cancellous bone and wood. *J Elast* 1998;53:125—46.
30. Sarikanat M, Yildiz H. Determination of bone density distribution in proximal femur by using the 3D orthotropic bone adaptation model. *J Eng Med* 2011;225(4):365—75.
31. Pietrzak G, Curnier A, Botsis J, Scherrer S, Wiskott A, Belser U. A nonlinear elastic model of the periodontal ligament and its numerical calibration for the study of tooth mobility. *Comput Methods Biomech Biomed Eng* 2002;5:91—100.
32. Roos-Jansaker AM, Renvert S, Egelberg J. Treatment of peri-implant infections: a literature review. *J Clin Periodontol* 2003;30:467—85.
33. Klineberg IJ, Trulsson M, Murray GM. Occlusion on implants - is there a problem? *J Oral Rehabil* 2012;39:522—37.
34. Ruimerman R. *Modeling and Remodeling in Bone Tissue*. Technische Universiteit Eindhoven Eindhoven, 2005.
35. Toms SR, Dakin GJ, Lemons JE, Eberhardt AW. Quasi-linear viscoelastic behavior of the human periodontal ligament. *J Biomech* 2002;35:1411—5.